



# Synthesis and evaluation of ursolic acid-based 1,2,4-triazolo[1,5-a]pyrimidines derivatives as anti-inflammatory agents

Tian-Yi Zhang<sup>1</sup> · Chun-Shi Li<sup>2</sup> · Ping Li<sup>1</sup> · Xue-Qian Bai<sup>1</sup> · Shu-Ying Guo<sup>1</sup> · Ying Jin<sup>1</sup> · Sheng-Jun Piao<sup>3</sup>

Received: 4 September 2020 / Accepted: 29 October 2020  
© Springer Nature Switzerland AG 2020

## Abstract

Here, two series of novel ursolic acid-based 1,2,4-triazolo[1,5-a]pyrimidines derivatives were synthesized and screened for their anti-inflammatory activity by evaluating their inhibition effect of using LPS-induced inflammatory response in RAW 264.7 macrophages in vitro; the effects of different concentrations of the compounds on the secretion of nitric oxide (NO) and inflammatory cytokines including TNF- $\alpha$  and IL-6 were evaluated. Their toxicity was also assessed in vitro. Results showed that the most prominent compound **3** could significantly decrease production of the above inflammatory factors. Docking study was performed for the representative compounds **3**, UA, and **Celecoxib** to explain their interaction with cyclooxygenase-2 (COX-2) receptor active site. In vitro enzyme study implied that compound **3** exerted its anti-inflammatory activity through COX-2 inhibition.

**Keywords** Ursolic acid · Anti-inflammatory activity · Molecular modeling · COX-2 inhibition

## Introduction

The inflammatory process is an immune response to a perturbation of the homeostatic equilibrium of the organism, whether endogenous or exogenous [1–3]. Inflammation can lead to further tissue damage that can eventually

contribute to the pathogenesis of chronic inflammatory and autoimmune diseases such as rheumatoid arthritis [4], cardiovascular diseases [5], CNS neurological disorders [6], and ulcerative colitis [7]. Management of inflammatory disorders involves the use of therapeutic agents for relieving pain and reducing inflammation, either decreasing or neutralizing the levels of pro-inflammatory mediators or inhibiting the recruitment of leukocytes and their activation. Nonsteroidal anti-inflammatory drugs (NSAIDs) are still widely used in clinical applications today. However, they usually cause unexpected side effects, such as peptic ulcers, bleeding, mucosal lesions, and nephrotoxicity [8, 9]. Traditional NSAIDs exhibit pharmacological action through the inhibition of cyclooxygenase (COX) activity in vivo and the reduction in the biosynthesis of prostaglandins in local tissues.

Pro-inflammatory cytokines also play an important role in the defense of disease [10, 11]. However, uncontrolled and excess release of pro-inflammatory mediators such as NO, tumor necrosis factor alpha (TNF- $\alpha$ ), and interleukin-6 (IL-6) can lead to multiple types of inflammatory diseases such as acute lung injury (ALI) [12–15].

Ursolic acid (UA) is a lipophilic pentacyclic triterpenoid found in a wide variety of plants and possesses a wide range of biological functions, such as anti-inflammation [16], anti-oxidation [17], and anti-fibrosis [18]. On the other hand,

---

Tian-Yi Zhang and Chun-Shi Li have contributed equally to this work.

**Electronic supplementary material** The online version of this article (<https://doi.org/10.1007/s11030-020-10154-7>) contains supplementary material, which is available to authorized users.

- 
- ✉ Tian-Yi Zhang  
tianyizhang@126.com
- ✉ Ying Jin  
jinying73@126.com
- ✉ Sheng-Jun Piao  
sjpiao8478@163.com

<sup>1</sup> Jilin Medical University, Jilin 132013, Jilin Province, People's Republic of China

<sup>2</sup> The Third People's Hospital of Dalian, Dalian 116000, Liaoning Province, People's Republic of China

<sup>3</sup> Department of General Surgery, Affiliated Hospital of Yanbian University, Yanji 133000, Jilin Province, People's Republic of China

1,2,4-triazolo[1,5-a] pyrimidines (TPs), a subtype of purine analogs, have been widely investigated and identified to possess diverse pharmacological properties. Huang et al. [19] showed that the steroidal containing 1,2,4-triazolo[1,5-a] pyrimidine moiety resulted in an enhancement of its anticancer activity, as exemplified by compounds **A** and **B** (Fig. 1). In the previous study, our group has designed and synthesized several effective ursolic acid derivatives bearing a 4-phenyl-1*H*-1,2,4-triazol-5(4*H*)-one or aminoguanidine moiety. Among them, compounds **C** and **D** (Fig. 1), which displayed the most potent anti-inflammatory activity of all of the compounds prepared, with 69.76% and 81.61% inhibition after intraperitoneal administration, respectively, were more potent than the reference drugs. In view of the pharmacological importance of ursolic acid and triazolo[1,5-a] pyrimidine functional group and in continuation of our previous work in developing new anti-inflammatory agents, a total of 23 target compounds were prepared (Fig. 2) and

evaluated for their anti-inflammatory activity *in vitro*. Subsequently, the preliminary action mechanism was also investigated in the present work.

## Results and discussion

### Chemistry

The synthetic pathway used for preparation of the target compounds **1–23** is outlined in Scheme 1. Intermediate **Z<sub>1</sub>** was prepared by reacting UA with Jones reagent in acetone. Compound **Z<sub>2</sub>** was synthesized by Claisen–Schmidt condensations between compound **Z<sub>1</sub>** and different aldehydes. Preparation of **Z<sub>3</sub>** was done according to a previously described method [20]. The target compounds **1–23** were subjected to aza-Michael addition reaction and intramolecular cyclization reaction with 3-amino-1,2,4-triazole subsequently in

**Fig. 1** Previously reported UA and TPs derivatives

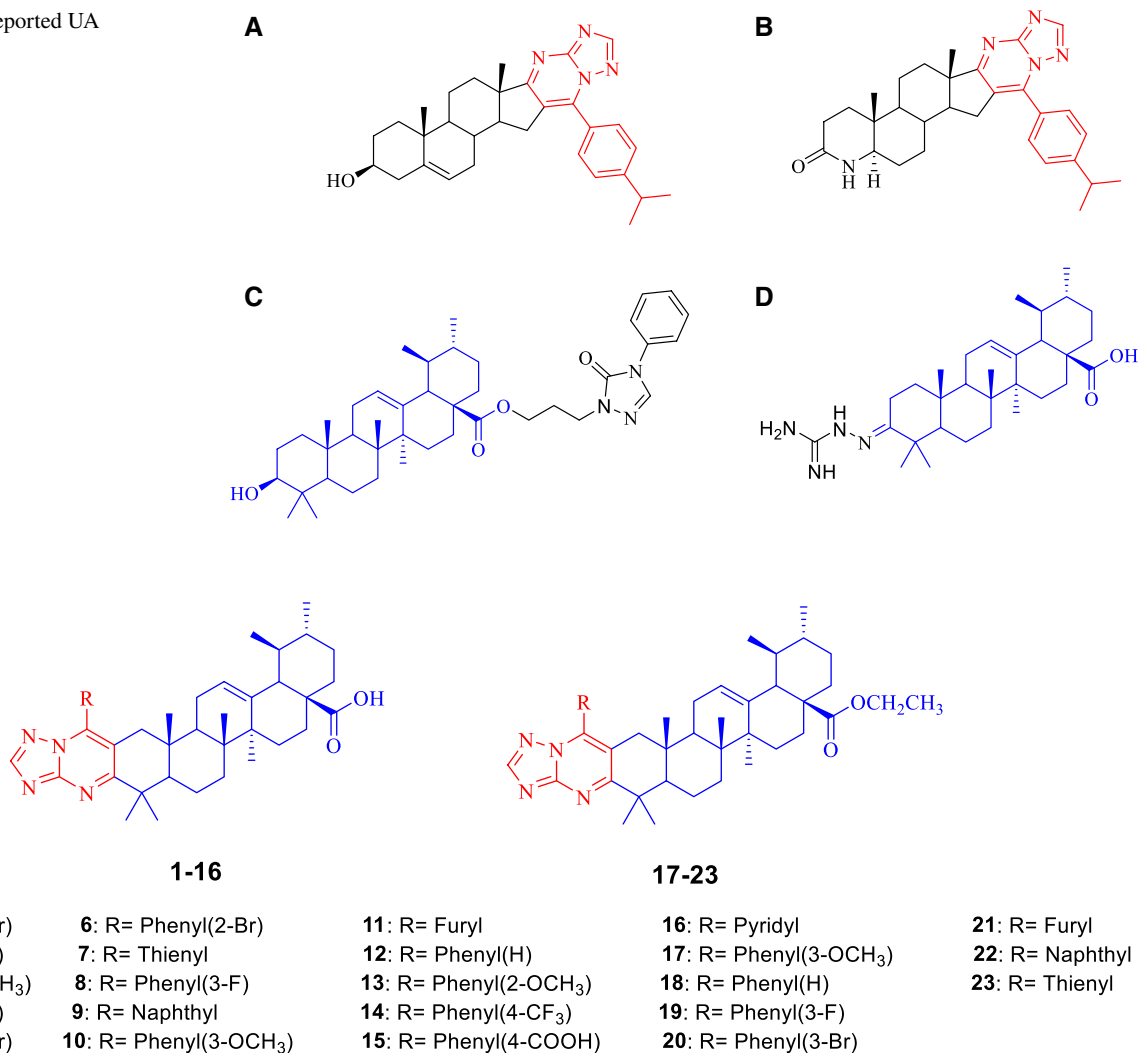
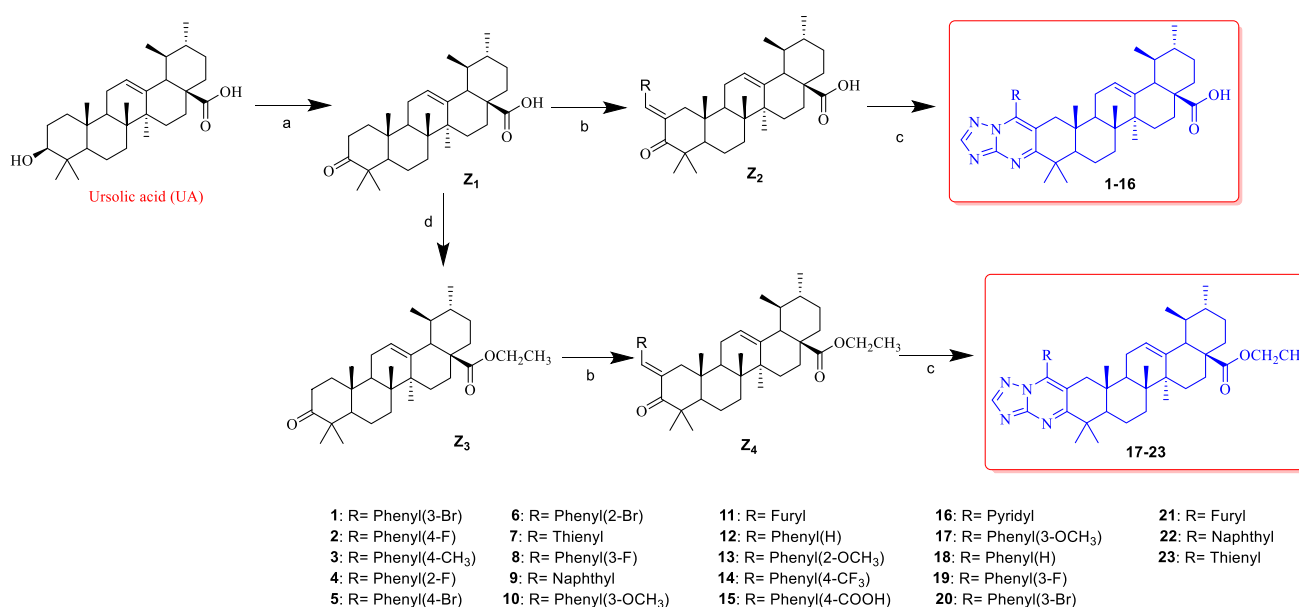


**Fig. 2** Synthesis of target compounds



**Scheme 1** Synthesis of the target compounds **1–23**. **a** Jones reagent, 0 °C, 5 h, 90%. **b** Aldehydes, 5% NaOH, ethanol, r.t., 2 h, 40–70%. **c** 3-amino-1,2,4-triazole, *n*-BuOH, reflux, 50–70%. **d** Iodoethane, K<sub>2</sub>CO<sub>3</sub>, DMF, r.t., 6 h, 40–60%

the presence of *t*-BuOK [19]. The final compounds were characterized by <sup>1</sup>H NMR, <sup>13</sup>C NMR, mass spectroscopy, and HRMS.

### Anti-inflammatory activity

The anti-inflammatory activity of the title compounds was tested applying a LPS-stimulated inflammation model. Because induced macrophages' cells death, if any occurs, would lead to a reduction in the measured production of cytokines (TNF- $\alpha$  and IL-6) in addition to nitric oxide regardless of the inhibition of activity, cell viability assay

was conducted to avoid inaccuracies arising from this factor. To investigate the relation between anti-inflammatory activity and cell viability for the compounds **1–23** and **24** (UA), the cytotoxic effects of these compounds were evaluated by MTT assay in RAW 264.7 cells. As presented in Fig. 3, most of the compounds showed low toxicity at 30  $\mu$ M. Compounds **1–6**, **9**, **10**, **12**, **15**, and **18–23** show weak cytotoxicity, which were lower than that of ursolic acid. Therefore, these compounds were found to be suitable for further evaluation.

Nitric oxide (NO) is a cell-signaling molecule that produces anti-inflammatory effects under normal

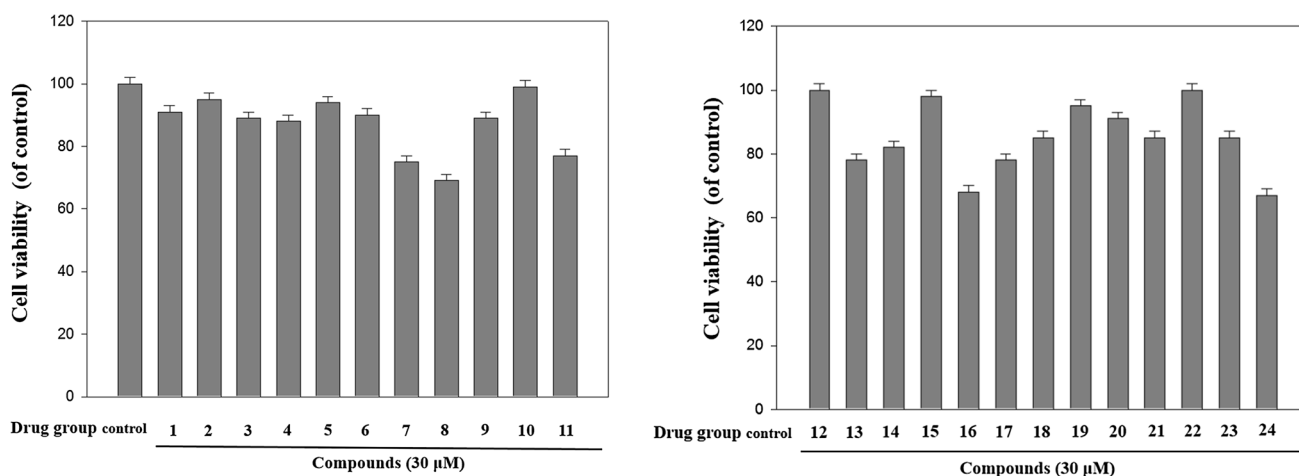


**Fig. 3** Cellular viability of compounds **1–24**. Data are shown as the mean  $\pm$  SD ( $n=3$ ) of three independent experiments

physiological conditions. High levels of NO are produced in response to LPS in the activated RAW 264.7 macrophages [21]. Therefore, NO inhibitors have been identified as potential agents for the treatment of inflammatory diseases [22]. In view of this, the inhibitory effects of compounds **1–6**, **9**, **10**, **12**, **15**, and **18–23** on LPS-induced production of the inflammatory mediators NO in RAW 264.7 cells were examined. Three different concentrations (3  $\mu\text{M}$ , 10  $\mu\text{M}$ , and 30  $\mu\text{M}$ ) of these compounds were used for the study. Dexamethasone (DXMS) was used as a positive control. One-way ANOVA followed by Dunnett's multiple comparison test was used to detect the significance. As shown in Fig. 4, the results demonstrated that compounds **2** and **3** could significantly inhibit NO production at 3  $\mu\text{M}$ , 10  $\mu\text{M}$ , and 30  $\mu\text{M}$  concentration levels in a dose-dependent manner. Compounds **2** and **3** showed significant NO production inhibitory effects at 30  $\mu\text{M}$ .

TNF- $\alpha$  has a wide range of biological activities, participates in inflammation and anti-tumor activities, and engages in the pathological process of endotoxin shock [23]. IL-6 is produced after TNF- $\alpha$  stimulation and is closely related to the pathological and physiological processes of various diseases [24]. Compounds **1–6**, **9**, **10**, **12**, **15**, and **18–23** were also evaluated for their activity against LPS-induced production of other inflammatory mediators, TNF- $\alpha$  and IL-6 in RAW 264.7 cells. Three different concentrations (3  $\mu\text{M}$ , 10  $\mu\text{M}$ , and 30  $\mu\text{M}$ ) of these compounds were measured. Dexamethasone (DXMS) was used as a positive control. As shown in Fig. 5, the results demonstrated that compounds **3**, **5**, **10**, **18**, **19**, **21**, and **22** showed significant TNF- $\alpha$  production inhibitory effects at 30  $\mu\text{M}$ . Compounds **3**, **5**, **9**, and **15** showed significant IL-6 production inhibitory effects at 30  $\mu\text{M}$ . These results

indicate the potential anti-inflammatory properties of the prepared compounds.

These studies revealed that the incorporation of a 1,2,4-triazolo[1,5-a]pyrimidines moiety to UA could provide unexpected improvement in the anti-inflammatory activity of UA derivatives. The previous study [20] showed that significant further improvement in the anti-inflammatory activity was observed while retaining the carboxylic acid functional group at the 17 position. Similar results were seen in our study, where compounds **3**, **5**, **9**, and **15** had more potent IL-6 inhibitory effects than compounds **18–23**, which had an ethyl group that was introduced at the 17-COOH position. However, there was no consistent trend observed for TNF- $\alpha$  inhibition by this class of compounds. The introduction of different substituents (differently substituted benzene rings, a naphthalene ring, and a heterocycle) to the C-2 of UA increased the anti-inflammatory activity. Furthermore, the replacement of the benzene rings derivatives at the *p*-position displayed higher potency, as exemplified by the compounds **2**, **3**, **5**, and **15**. No clear pattern was found for the structure/activity relationship between the anti-inflammatory activity and physicochemical properties of different substituents on the phenyl ring, indicating that the electronic effect of the substituent on the benzene ring is not critical. Based on the above, compound **3** was found to be the most prominent one. Thus, compound **3** was used as the main compound for mechanism exploration of action.

## Molecular docking

Wei et al. [25] reported that the UA derivatives exhibited high affinity for the COX-2 active site and possibly exhibit their anti-inflammatory potency via inhibiting COX-2

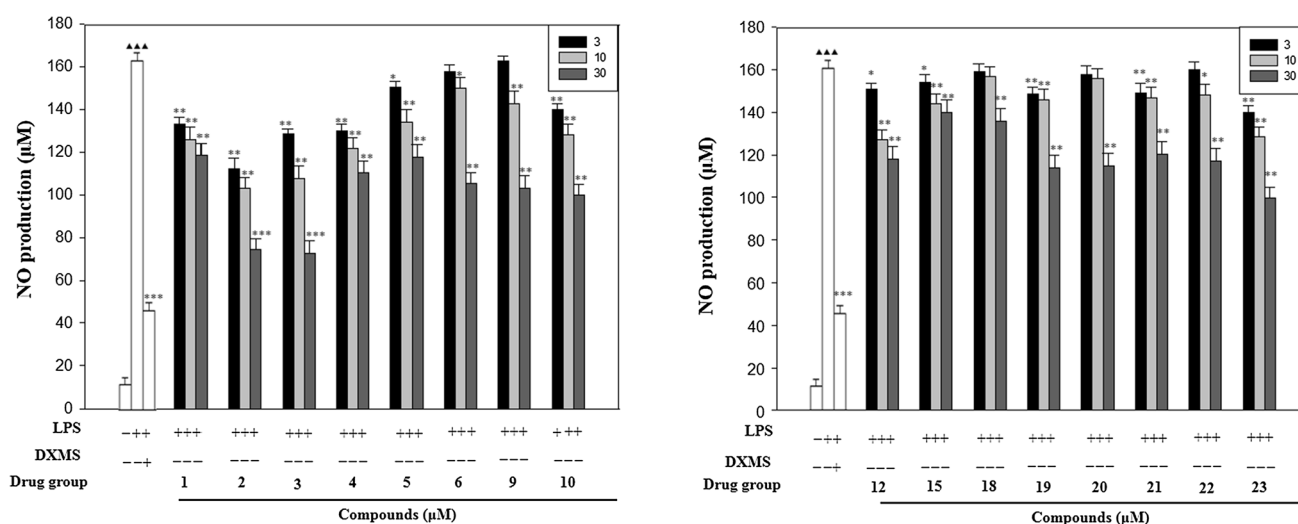


**Fig. 4** The NO inhibitory effects of compounds **1–6**, **9**, **10**, **12**, **15**, and **18–23**. Data are shown as the mean  $\pm$  SD ( $n=3$ ) of three independent experiments. \* $p < 0.05$ , \*\* $p < 0.01$ , \*\*\* $p < 0.001$ , significant with respect to the control

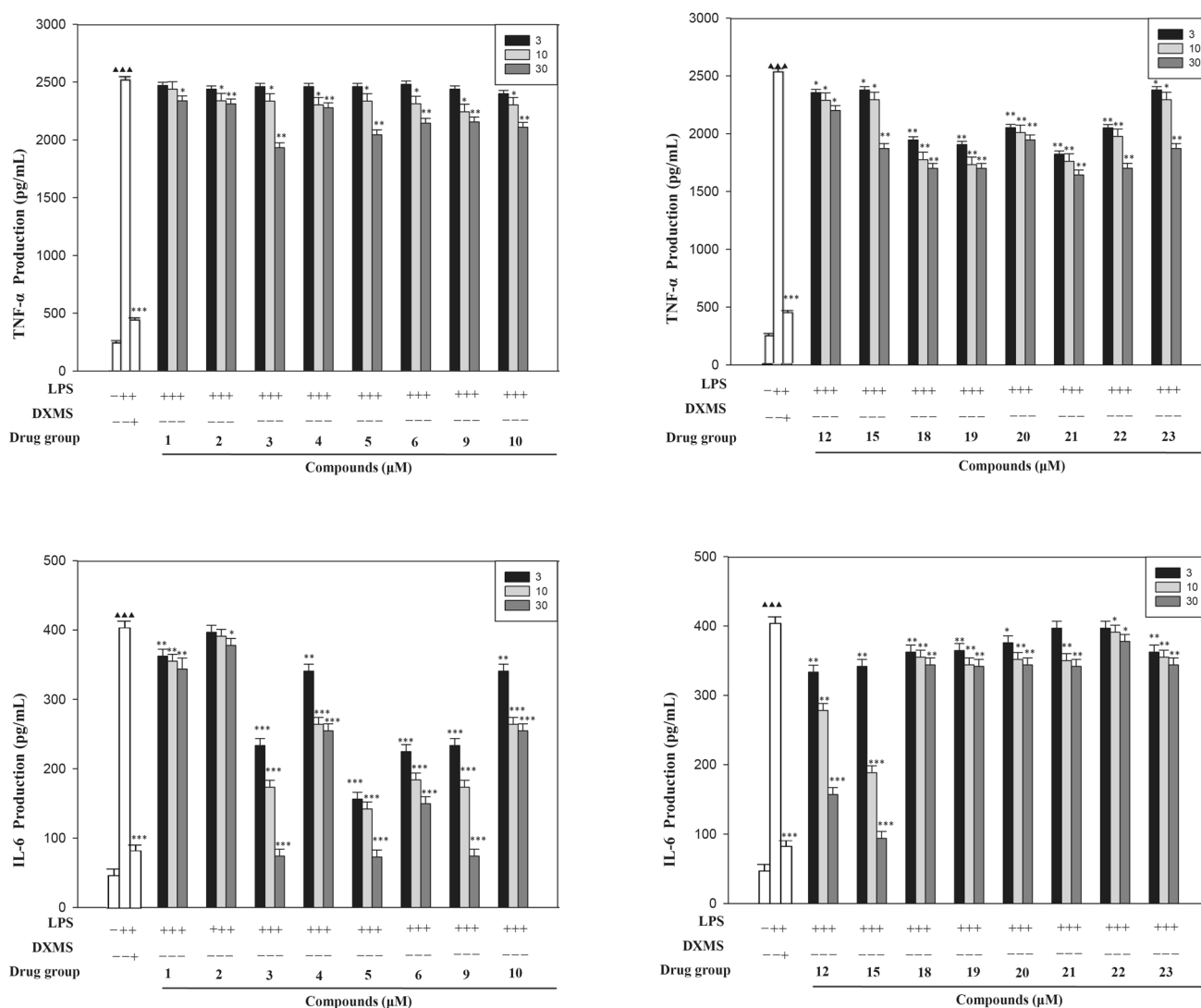


**Fig. 5** The TNF- $\alpha$  and IL-6 inhibitory effects of compounds 1–6, 9, 10, 12, 15, and 18–23. Data are shown as the mean  $\pm$  SD ( $n=3$ ) of three independent experiments. \* $p < 0.05$ , \*\* $p < 0.01$ , \*\*\* $p < 0.001$ , significant with respect to the control

enzymes. The molecular docking analysis of compound **3**, UA, and **Celecoxib** was carried out to elucidate their anti-inflammatory activity in vitro. The scoring functions and hydrogen bonds formed with the surrounding amino acids were used to explore the binding modes, binding affinities, and orientations of the docked compounds at the active site of COX-2 enzyme. The crystal structure of the COX-2 enzyme obtained from the protein data bank (PDB ID: 5FDQ) was used for the molecular docking studies. The binding mode and the protein–ligand interactions of compound **3**, UA, and **Celecoxib** are depicted in Fig. 6. The binding mode of the most active compound **3** simulates certain key interactions with the reference drug **Celecoxib**. The result shows that compound **3** may bind well to the COX-2 protein and while interacting with

Val444 (4.33 Å and 3.95 Å), Val447 (5.35 Å and 4.51 Å), Ala202 (6.48 Å), Tyr385 (4.58 Å), and His207 (5.19 Å and 5.35 Å), respectively. UA showed interaction with Val447 (5.43 Å and 4.20 Å), Trp387 (2.01 Å), Tyr385 (4.49 Å), His388 (4.46 Å), His386 (4.64 Å) and His207 (5.28 Å and 4.39 Å), respectively. Furthermore, compound **3** presented better anti-inflammatory activity and showed higher docking scores (145.52 kcal/mol) compared to UA (106.12 kcal/mol). The results of preliminary docking studies suggested that compound **3** possibly shows its anti-inflammatory activity through the interaction with COX-2 protein by targeting residues in the active cavities of COX-2.



## COX-2 enzymatic activity

According to the docking study, the inhibitory effect on COX-2 enzyme produced by the compound **3** represents a possible mechanism of action for their strong anti-inflammatory activity. In order to verify our speculation, the effect of compound **3** on COX-2 enzyme was evaluated. The production of COX-2 was determined by enzyme-linked immunosorbent assay (ELISA) [26]. Celecoxib and UA were used as a positive control. Five different concentrations (0.1  $\mu\text{M}$ , 0.3  $\mu\text{M}$ , 1  $\mu\text{M}$ , 3  $\mu\text{M}$ , and 10  $\mu\text{M}$ ) of compounds **3**, Celecoxib, and UA were measured. As shown in Fig. 7, the results showed a dose-dependent decrease in COX-2 production in the presence of compounds **3**, Celecoxib, and UA. The 10  $\mu\text{M}$  concentration of compound **3** decreased the COX-2 activity by 54% when compared with the negative control. The COX-2 inhibitory activity of compound **3** was slightly lower than the activity of reference drug Celecoxib. To sum up, in vitro enzyme study implied that compound **3** exerted its anti-inflammatory activity through COX-2 enzyme inhibition.

## Conclusions

In this report, two series of novel ursolic acid-based 1,2,4-triazolo[1,5-a]pyrimidines derivatives were synthesized and evaluated for their anti-inflammatory activity. Compound **3** exerted anti-inflammatory activity through suppressing of the expression of pro-inflammatory factors, including NO, TNF- $\alpha$ , and IL-6 in LPS-stimulated RAW 264.7 macrophages. The molecular docking study results indicated that the compound **3** exhibited high affinity for the COX-2 active site and possibly exhibited its

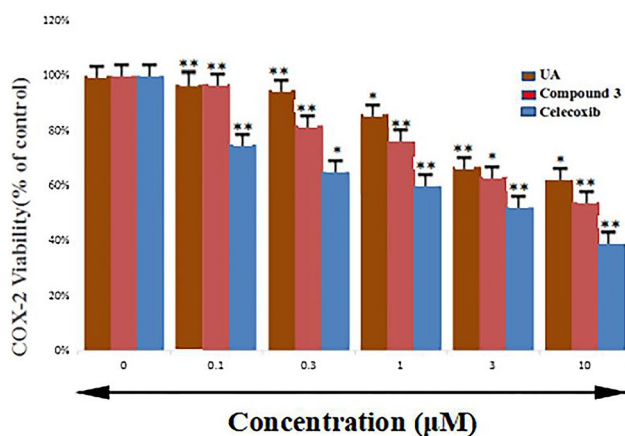


**Fig. 7** Inhibition of COX-2 activities of compounds **3**, UA, and Celecoxib. Data are shown as the mean  $\pm$  SD ( $n=3$ ) of three independent experiments. \* $p < 0.05$ , \*\* $p < 0.01$ , significant with respect to the control

anti-inflammatory potency via inhibiting COX-2 enzyme. The COX-2 inhibitory activity of compound **3** was slightly lower in magnitude compared to the reference drug Celecoxib. Combination of all the results obtained in the present study establishes the therapeutic potential of compound **3** and presents it as a potential anti-inflammatory lead.

## Experimental section

Silica gel thin-layer chromatography (TLC) plates (Qing Dao Marine Chemical Factory, Qingdao, China) were used to monitor the reaction progress. Developed plates were examined with UV lamps at wavelengths of 254 nm. Nuclear magnetic resonance spectra were measured on an AV-300 or AV-500 spectrometer (Bruker, Zurich, Switzerland) operating at 300 MHz for  $^1\text{H}$  and 126 MHz for  $^{13}\text{C}$  NMR while using TMS as the internal standard. Mass spectra were measured on a MALDI-TOF (Shimadzu, Japan). HRMS was measured on a Thermo Scientific LTQ Orbitrap XL spectrometer. All commercial chemicals were used as supplied unless otherwise indicated.

### General synthetic procedure for the intermediates **Z**<sub>1</sub>, **Z**<sub>2</sub>, **Z**<sub>3</sub>, and **Z**<sub>4</sub>

Intermediates **Z**<sub>1</sub>, **Z**<sub>2</sub>, **Z**<sub>3</sub>, and **Z**<sub>4</sub> were synthesized using the reported procedure [20].

### General synthetic procedure for the target compounds **1–23**

The intermediate **Z**<sub>2</sub> or **Z**<sub>4</sub> (1.0 mmol) was dissolved in *n*-BuOH (20 mL). To the solution was added 3-amino-1,2,4-triazole (4.0 mmol) and *t*-BuOK (4.0 mmol). The resulting mixture was refluxed for about 24 h. After removal of the solvent, the residue was purified by silica gel chromatography using dichloromethane/methanol (15/1) as the eluent to give the target compounds **1–23**.

(1*S*,2*R*,4*aS*,6*aS*,6*bR*,16*aR*)-15-(3-Bromophenyl)-1,2,6*a*,6*b*,9,9,16*a*-heptamethyl-1,3,4,5,6,6*a*,6*b*,7,8,8*a*,9,16,16*a*,16*b*,17,18*b*-hexadecahydrochryseno[1,2-*g*][1,2,4]triazolo[5,1-*b*]quinazoline-4*a*(2*H*)-carboxylic acid (**1**) White solid. Yield 48%, m.p. 185–187  $^{\circ}\text{C}$ .  $^1\text{H}$  NMR (300 MHz,  $\text{CDCl}_3$ )  $\delta$  9.97 (s, 1H), 7.54 (d,  $J=4.2$  Hz, 1H), 7.35 (s, 1H), 7.07 (d,  $J=7.1$  Hz, 1H), 6.91 (s, 1H), 5.55 (d,  $J=14.2$  Hz, 1H), 5.30 (s, 1H), 2.19–0.64 (m, 42H, protons in UA skeleton).  $^{13}\text{C}$  NMR (126 MHz,  $\text{CDCl}_3$ )  $\delta$  175.67, 149.58, 148.58, 142.19, 138.16, 134.90, 131.61, 130.90, 130.16, 125.36, 122.84, 63.18, 53.42, 50.86, 48.01, 42.07, 39.43, 35.72, 29.71,

27.81, 23.20, 20.60, 18.67, 16.64, 14.96. MS (MALDI-TOF)  $m/z$  685 ( $M^+ + H$ ).

**(1S,2R,4aS,6aS,6bR,16aR)-15-(4-Fluorophenyl)-1,2,6a,6b,9,9,16a-heptamethyl-1,3,4,5,6,6a,6b,7,8,8a,9,16,16a,16b,17,18b-hexadecahydrochryseno[1,2-g][1,2,4]triazolo[5,1-b]quinazoline-4a(2H)-carboxylic acid (2)** White solid. Yield 52%, m.p. 140–142 °C.  $^1H$  NMR (300 MHz,  $CDCl_3$ )  $\delta$  8.39 (d,  $J = 12.0$  Hz, 1H), 7.56 (s, 1H), 7.28 (s, 1H), 7.17 (s, 1H), 6.95 (s, 1H), 5.62 (s, 1H), 5.22 (d,  $J = 10.2$  Hz, 1H), 2.71–0.64 (m, 42H, protons in UA skeleton).  $^{13}C$  NMR (126 MHz,  $CDCl_3$ )  $\delta$  170.27, 129.36, 125.37, 125.25, 125.12, 124.90, 116.56, 116.25, 115.74, 115.64, 115.46, 48.00, 42.42, 42.14, 39.49, 39.19, 38.87, 36.77, 35.95, 35.74, 32.39, 30.70, 29.72, 29.41, 29.26, 29.08, 28.61, 28.42, 28.09, 24.25, 23.48, 23.17, 21.16, 20.45, 18.67, 15.02, 14.18. MS (MALDI-TOF)  $m/z$  625 ( $M^+ + H$ ).

**(1S,2R,4aS,6aS,6bR,16aR)-1,2,6a,6b,9,9,16a-Heptamethyl-15-(p-tolyl)-1,3,4,5,6,6a,6b,7,8,8a,9,16,16a,16b,17,18b-hexadecahydrochryseno[1,2-g][1,2,4]triazolo[5,1-b]quinazoline-4a(2H)-carboxylic acid (3)** White solid. Yield 52%, m.p. 194–196 °C.  $^1H$  NMR (300 MHz,  $CDCl_3$ )  $\delta$  10.99 (s, 1H), 8.39 (s, 1H), 7.42 (s, 2H), 7.17 (d,  $J = 8.1$  Hz, 1H), 7.11 (d,  $J = 8.0$  Hz, 1H), 5.58 (s, 1H), 2.50 (s, 3H), 2.77–0.80 (m, 42H, protons in UA skeleton).  $^{13}C$  NMR (126 MHz,  $CDCl_3$ )  $\delta$  183.01, 174.39, 154.09, 145.79, 141.13, 138.33, 129.81, 129.19, 125.87, 125.11, 117.32, 53.09, 52.71, 47.98, 45.29, 42.21, 41.85, 41.47, 40.27, 39.44, 39.07, 38.82, 36.67, 36.12, 32.32, 32.22, 27.96, 25.12, 23.49, 23.29, 21.66, 20.27. MS (MALDI-TOF)  $m/z$  621 ( $M^+ + H$ ). HRMS (ESI)  $m/z$  calcd for  $C_{40}H_{53}N_4O_2^+$  ( $M + H$ ) $^+$  621.41630, found 621.41589.

**(1S,2R,4aS,6aS,6bR,16aR)-15-(2-Fluorophenyl)-1,2,6a,6b,9,9,16a-heptamethyl-1,3,4,5,6,6a,6b,7,8,8a,9,16,16a,16b,17,18b-hexadecahydrochryseno[1,2-g][1,2,4]triazolo[5,1-b]quinazoline-4a(2H)-carboxylic acid (4)** White solid. Yield 46%, m.p. 164–166 °C.  $^1H$  NMR (300 MHz,  $CDCl_3$ )  $\delta$  10.33 (s, 1H), 7.57 (s, 1H), 7.26 (s, 1H), 7.12 (s, 1H), 6.91 (s, 1H), 6.06 (s, 1H), 5.18 (s, 1H), 2.72–0.59 (m, 42H, protons in UA skeleton).  $^{13}C$  NMR (126 MHz,  $CDCl_3$ )  $\delta$  176.65, 150.15, 148.51, 138.08, 134.85, 130.92, 130.01, 129.19, 128.85, 126.83, 125.44, 124.34, 115.51, 99.35, 65.58, 50.83, 48.02, 45.75, 42.02, 39.39, 39.02, 38.85, 35.63, 30.59, 28.68, 27.74, 21.15, 20.30, 19.66, 19.20, 16.95, 16.51, 14.87. MS (MALDI-TOF)  $m/z$  625 ( $M^+ + H$ ).

**(1S,2R,4aS,6aS,6bR,16aR)-15-(4-Bromophenyl)-1,2,6a,6b,9,9,16a-heptamethyl-1,3,4,5,6,6a,6b,7,8,8a,9,16,16a,16b,17,18b-hexadecahydrochryseno[1,2-g][1,2,4]triazolo[5,1-b]quinazoline-4a(2H)-carboxylic acid (5)** White solid. Yield 48%, m.p. 172–174 °C.  $^1H$  NMR (300 MHz,  $CDCl_3$ )  $\delta$  9.98 (s, 1H), 7.60 (s, 1H), 7.32 (d,  $J = 7.5$  Hz, 1H), 7.26 (s, 1H), 7.03

(d,  $J = 8.2$  Hz, 1H), 5.59 (s, 1H), 5.19 (s, 1H), 2.73–0.57 (m, 42H, protons in UA skeleton).  $^{13}C$  NMR (126 MHz,  $CDCl_3$ )  $\delta$  172.30, 138.96, 138.10, 134.42, 132.42, 131.75, 131.13, 130.97, 129.27, 125.34, 122.52, 40.62, 40.52, 39.39, 38.84, 35.99, 35.68, 32.21, 29.71, 28.61, 23.96, 23.55, 23.18, 21.15, 20.48, 16.93, 16.65, 14.97. MS (MALDI-TOF)  $m/z$  685 ( $M^+ + H$ ).

**(1S,2R,4aS,6aS,6bR,16aR)-15-(2-Bromophenyl)-1,2,6a,6b,9,9,16a-heptamethyl-1,3,4,5,6,6a,6b,7,8,8a,9,16,16a,16b,17,18b-hexadecahydrochryseno[1,2-g][1,2,4]triazolo[5,1-b]quinazoline-4a(2H)-carboxylic acid (6)** White solid. Yield 42%, m.p. 177–179 °C.  $^1H$  NMR (300 MHz,  $CDCl_3$ )  $\delta$  10.38 (s, 1H), 7.75 (s, 1H), 7.57 (s, 1H), 7.26 (s, 1H), 6.96 (d,  $J = 6.9$  Hz, 1H), 6.36 (s, 1H), 5.19 (s, 1H), 2.69–0.55 (m, 42H, protons in UA skeleton).  $^{13}C$  NMR (126 MHz,  $CDCl_3$ )  $\delta$  178.60, 150.16, 149.86, 148.77, 148.42, 139.45, 139.33, 138.08, 138.03, 134.74, 134.55, 132.60, 132.53, 129.83, 129.72, 125.52, 125.43, 53.41, 50.85, 48.01, 45.80, 39.04, 38.87, 36.00, 35.62, 29.71, 28.73, 27.81, 27.68, 14.91. MS (MALDI-TOF)  $m/z$  686 ( $M^+ + 2$ ).

**(1S,2R,4aS,6aS,6bR,16aR)-1,2,6a,6b,9,9,16a-Heptamethyl-15-(thiophen-2-yl)-1,3,4,5,6,6a,6b,7,8,8a,9,16,16a,16b,17,18b-hexadecahydrochryseno[1,2-g][1,2,4]triazolo[5,1-b]quinazoline-4a(2H)-carboxylic acid (7)** White solid. Yield 54%, m.p. 211–213 °C.  $^1H$  NMR (300 MHz,  $CDCl_3$ )  $\delta$  9.79 (s, 1H), 7.54 (s, 1H), 7.14 (s, 1H), 7.04 (d,  $J = 3.0$  Hz, 1H), 5.94 (s, 1H), 5.20 (s, 1H), 2.46–0.75 (m, 42H, protons in UA skeleton).  $^{13}C$  NMR (126 MHz,  $CDCl_3$ )  $\delta$  172.40, 148.04, 147.82, 143.59, 138.13, 134.55, 133.11, 130.56, 127.20, 127.01, 126.55, 126.19, 125.45, 53.41, 50.82, 48.02, 45.98, 42.15, 40.86, 39.48, 38.88, 36.01, 35.82, 32.31, 30.67, 28.64, 19.64, 16.95, 15.33. MS (MALDI-TOF)  $m/z$  613 ( $M^+ + H$ ).

**(1S,2R,4aS,6aS,6bR,16aR)-15-(3-Fluorophenyl)-1,2,6a,6b,9,9,16a-heptamethyl-1,3,4,5,6,6a,6b,7,8,8a,9,16,16a,16b,17,18b-hexadecahydrochryseno[1,2-g][1,2,4]triazolo[5,1-b]quinazoline-4a(2H)-carboxylic acid (8)** White solid. Yield 52%, m.p. 198–200 °C.  $^1H$  NMR (300 MHz,  $CDCl_3$ )  $\delta$  9.67 (s, 1H), 8.36 (s, 1H), 7.62 (s, 1H), 7.26 (s, 1H), 7.06–6.84 (m, 2H), 5.20 (s, 1H), 2.65–0.65 (m, 42H, protons in UA skeleton).  $^{13}C$  NMR (126 MHz,  $CDCl_3$ )  $\delta$  182.13, 173.51, 155.64, 138.48, 138.11, 131.05, 130.94, 125.00, 123.51, 123.41, 117.92, 117.66, 116.76, 115.88, 115.56, 114.78, 114.50, 42.28, 42.12, 41.44, 39.45, 39.12, 36.70, 36.15, 35.98, 35.73, 30.66, 28.59, 28.04, 25.15, 23.50, 20.35, 19.59, 17.10, 16.94, 15.03. MS (MALDI-TOF)  $m/z$  625 ( $M^+ + H$ ). HRMS (ESI)  $m/z$  calcd for  $C_{39}H_{50}FN_4O_2^+$  ( $M + H$ ) $^+$  625.39123, found 625.39124.

**(1S,2R,4aS,6aS,6bR,16aR)-1,2,6a,6b,9,9,16a-Heptamethyl-15-(naphthalen-2-yl)-1,3,4,5,6,6a,6b,7,8,8a,9,16,16a,16b,17,18b-hexadecahydrochryseno[1,2-g][1,2,4]triazolo[5,1-b]quinazoline-4a(2H)-carboxylic acid (9)** White solid. Yield 52%, m.p. 110–112 °C.  $^1\text{H}$  NMR (300 MHz,  $\text{CDCl}_3$ )  $\delta$  9.77 (s, 1H), 8.35 (s, 1H), 8.09 (d,  $J=8.9$  Hz, 1H), 7.98 (d,  $J=6.4$  Hz, 1H), 7.88–7.74 (m, 2H), 7.66–7.57 (m, 1H), 7.52 (d,  $J=3.9$  Hz, 1H), 7.23 (d,  $J=8.4$  Hz, 1H), 5.11 (s, 1H), 2.77–0.63 (m, 42H, protons in UA skeleton).  $^{13}\text{C}$  NMR (126 MHz,  $\text{CDCl}_3$ )  $\delta$  173.51, 138.07, 138.01, 133.48, 133.44, 132.98, 132.95, 130.94, 130.90, 128.77, 128.71, 128.23, 128.12, 127.82, 127.74, 127.57, 127.49, 127.03, 126.96, 125.38, 125.31, 124.46, 124.42, 42.17, 41.44, 39.43, 39.11, 38.84, 36.00, 35.77, 30.68, 29.11, 23.25, 23.17, 20.56, 20.48, 19.60, 19.56, 16.75. MS (MALDI-TOF)  $m/z$  657 ( $\text{M}^+ + \text{H}$ ).

**(1S,2R,4aS,6aS,6bR,16aR)-15-(3-Methoxyphenyl)-1,2,6a,6b,9,9,16a-heptamethyl-1,3,4,5,6,6a,6b,7,8,8a,9,16,16a,16b,17,18b-hexadecahydrochryseno[1,2-g][1,2,4]triazolo[5,1-b]quinazoline-4a(2H)-carboxylic acid (10)** White solid. Yield 48%, m.p. 178–180 °C.  $^1\text{H}$  NMR (300 MHz,  $\text{CDCl}_3$ )  $\delta$  9.48 (s, 1H), 7.54 (s, 1H), 7.17 (s, 1H), 6.88 (s, 1H), 6.79 (s, 1H), 5.54 (s, 1H), 5.20 (s, 1H), 3.88 (s, 3H), 3.77–0.75 (m, 42H, protons in UA skeleton). MS (MALDI-TOF)  $m/z$  637 ( $\text{M}^+ + \text{H}$ ).

**(1S,2R,4aS,6aS,6bR,16aR)-15-(Furan-2-yl)-1,2,6a,6b,9,9,16a-heptamethyl-1,3,4,5,6,6a,6b,7,8,8a,9,16,16a,16b,17,18b-hexadecahydrochryseno[1,2-g][1,2,4]triazolo[5,1-b]quinazoline-4a(2H)-carboxylic acid (11)** White solid. Yield 48%, m.p. 185–187 °C.  $^1\text{H}$  NMR (300 MHz,  $\text{CDCl}_3$ )  $\delta$  8.76 (s, 1H), 7.57 (s, 1H), 7.31 (d,  $J=5.5$  Hz, 1H), 6.39 (d,  $J=2.8$  Hz, 1H), 5.74 (s, 1H), 5.23 (s, 1H), 2.20–0.76 (m, 42H, protons in UA skeleton).  $^{13}\text{C}$  NMR (126 MHz,  $\text{CDCl}_3$ )  $\delta$  180.94, 154.94, 151.03, 145.69, 143.05, 138.23, 120.74, 112.32, 110.46, 109.76, 45.90, 45.72, 42.40, 41.38, 40.99, 39.54, 39.45, 38.96, 36.85, 36.00, 35.88, 32.77, 32.32, 28.43, 24.89, 23.24, 23.20. MS (MALDI-TOF)  $m/z$  597 ( $\text{M}^+ + \text{H}$ ). HRMS (ESI)  $m/z$  calcd for  $\text{C}_{37}\text{H}_{49}\text{N}_4\text{O}_3^+$  ( $\text{M} + \text{H}$ ) $^+$  597.37992, found 597.37927.

**(1S,2R,4aS,6aS,6bR,16aR)-1,2,6a,6b,9,9,16a-Heptamethyl-15-phenyl-1,3,4,5,6,6a,6b,7,8,8a,9,16,16a,16b,17,18b-hexadecahydrochryseno[1,2-g][1,2,4]triazolo[5,1-b]quinazoline-4a(2H)-carboxylic acid (12)** White solid. Yield 50%, m.p. 216–218 °C.  $^1\text{H}$  NMR (300 MHz,  $\text{CDCl}_3$ )  $\delta$  10.13 (s, 1H), 7.56 (s, 1H), 7.26 (s, 1H), 7.14 (s, 3H), 5.60 (s, 1H), 5.16 (s, 1H), 2.72–0.60 (m, 42H, protons in UA skeleton).  $^{13}\text{C}$  NMR (126 MHz,  $\text{CDCl}_3$ )  $\delta$  180.34, 154.50, 137.07, 129.57, 128.31, 128.05, 127.62, 126.63, 124.37, 51.78, 49.79, 46.96, 41.10, 38.43, 38.08, 37.84, 35.75, 35.08, 31.35, 29.65, 27.58, 26.96, 23.10, 22.48, 22.20, 20.13,

19.43, 18.58, 15.95, 15.83, 13.99. MS (MALDI-TOF)  $m/z$  607 ( $\text{M}^+ + \text{H}$ ).

**(1S,2R,4aS,6aS,6bR,16aR)-15-(2-Methoxyphenyl)-1,2,6a,6b,9,9,16a-heptamethyl-1,3,4,5,6,6a,6b,7,8,8a,9,16,16a,16b,17,18b-hexadecahydrochryseno[1,2-g][1,2,4]triazolo[5,1-b]quinazoline-4a(2H)-carboxylic acid (13)** White solid. Yield 50%, m.p. 220–221 °C.  $^1\text{H}$  NMR (300 MHz,  $\text{CDCl}_3$ )  $\delta$  9.26 (s, 1H), 8.32 (s, 1H), 7.52 (s, 1H), 7.20 (d,  $J=7.2$  Hz, 1H), 7.05 (s, 1H), 6.84 (d,  $J=8.2$  Hz, 1H), 5.18 (s, 1H), 3.74 (s, 3H), 2.62–0.58 (m, 42H, protons in UA skeleton). MS (MALDI-TOF)  $m/z$  637 ( $\text{M}^+ + \text{H}$ ).

**(1S,2R,4aS,6aS,6bR,16aR)-1,2,6a,6b,9,9,16a-Heptamethyl-15-(4-(trifluoromethyl)phenyl)-1,3,4,5,6,6a,6b,7,8,8a,9,16,16a,16b,17,18b-hexadecahydrochryseno[1,2-g][1,2,4]triazolo[5,1-b]quinazoline-4a(2H)-carboxylic acid (14)** White solid. Yield 50%, m.p. 203–205 °C.  $^1\text{H}$  NMR (300 MHz,  $\text{CDCl}_3$ )  $\delta$  10.01 (s, 1H), 7.58 (s, 2H), 7.49 (s, 2H), 5.69 (s, 1H), 5.18 (s, 1H), 2.67–0.56 (m, 42H, protons in UA skeleton).  $^{13}\text{C}$  NMR (126 MHz,  $\text{CDCl}_3$ )  $\delta$  175.90, 143.71, 143.45, 138.20, 134.69, 130.03, 128.02, 126.26, 126.09, 125.68, 125.22, 125.00, 124.84, 45.83, 42.13, 40.62, 39.40, 39.06, 38.84, 36.74, 36.01, 35.71, 30.65, 28.52, 27.87, 24.11, 23.94, 23.47, 23.12, 21.13, 20.44, 19.54. MS (MALDI-TOF)  $m/z$  675 ( $\text{M}^+ + \text{H}$ ). HRMS (ESI)  $m/z$  calcd for  $\text{C}_{40}\text{H}_{50}\text{F}_3\text{N}_4\text{O}_2^+$  ( $\text{M} + \text{H}$ ) $^+$  675.38804, found 675.38721.

**(1S,2R,4aS,6aS,6bR,16aR)-15-(4-Carboxyphenyl)-1,2,6a,6b,9,9,16a-heptamethyl-1,3,4,5,6,6a,6b,7,8,8a,9,16,16a,16b,17,18b-hexadecahydrochryseno[1,2-g][1,2,4]triazolo[5,1-b]quinazoline-4a(2H)-carboxylic acid (15)** White solid. Yield 48%, m.p. 227–229 °C.  $^1\text{H}$  NMR (300 MHz, DMSO)  $\delta$  12.17 (s, 2H), 9.36 (s, 1H), 8.26–8.04 (m, 1H), 7.91 (d,  $J=8.2$  Hz, 1H), 7.52 (s, 1H), 7.29 (s, 1H), 5.13 (s, 1H), 2.09–0.77 (m, 42H, protons in UA skeleton). MS (MALDI-TOF)  $m/z$  651 ( $\text{M}^+ + \text{H}$ ).

**(1S,2R,4aS,6aS,6bR,16aR)-1,2,6a,6b,9,9,16a-Heptamethyl-15-(pyridin-3-yl)-1,3,4,5,6,6a,6b,7,8,8a,9,16,16a,16b,17,18b-hexadecahydrochryseno[1,2-g][1,2,4]triazolo[5,1-b]quinazoline-4a(2H)-carboxylic acid (16)** White solid. Yield 46%, m.p. 221–223 °C.  $^1\text{H}$  NMR (300 MHz,  $\text{CDCl}_3$ )  $\delta$  8.57 (d,  $J=12.0$  Hz, 1H), 7.62 (s, 1H), 7.55 (d,  $J=8.4$  Hz, 1H), 5.67 (s, 1H), 5.21 (d,  $J=14.0$  Hz, 1H), 2.38–0.62 (m, 42H, protons in UA skeleton). MS (MALDI-TOF)  $m/z$  608 ( $\text{M}^+ + \text{H}$ ).

**Ethyl(1S,2R,4aS,6aS,6bR,16aR)-15-(3-methoxyphenyl)-1,2,6a,6b,9,9,16a-heptamethyl-1,3,4,5,6,6a,6b,7,8,8a,9,16,16a,16b,17,18b-hexadecahydrochryseno[1,2-g][1,2,4]triazolo[5,1-b]quinazoline-4a(2H)-carboxylate (17)** White solid. Yield 52%, m.p. 109–110 °C.  $^1\text{H}$  NMR (300 MHz, DMSO)  $\delta$

7.45 (d,  $J=7.8$  Hz, 1H), 7.19–7.05 (m, 3H), 5.76 (s, 1H), 5.15 (s, 1H), 4.12 (q,  $J=9.4$  Hz, 2H), 3.80 (s, 3H), 3.51 (s, 3H), 2.46–0.70 (m, 42H, protons in UA skeleton). MS (MALDI-TOF)  $m/z$  665 ( $M^+ + H$ ). HRMS (ESI)  $m/z$  calcd for  $C_{42}H_{57}N_4O_3^+$  ( $M + H$ )<sup>+</sup> 665.44252, found 665.44183.

**Ethyl(1S,2R,4aS,6aS,6bR,16aR)-1,2,6a,6b,9,9,16a-heptamethyl-15-phenyl-1,3,4,5,6,6a,6b,7,8,8a,9,16,16a,16b,17,18b-hexadecahydrochryseno[1,2-g][1,2,4]triazolo[5,1-b]quinazoline-4a(2H)-carboxylate (18)** White solid. Yield 48%, m.p. 112–114 °C. <sup>1</sup>H NMR (300 MHz, DMSO)  $\delta$  7.59 (d,  $J=1.6$  Hz, 2H), 7.53 (m, 3H), 5.76 (s, 1H), 5.14 (s, 1H), 4.14 (q,  $J=9.8$  Hz, 2H), 3.51 (s, 3H), 2.53–0.70 (m, 42H, protons in UA skeleton). MS (MALDI-TOF)  $m/z$  635 ( $M^+ + H$ ). HRMS (ESI)  $m/z$  calcd for  $C_{41}H_{55}N_4O_2^+$  ( $M + H$ )<sup>+</sup> 635.43195, found 635.43176.

**Ethyl(1S,2R,4aS,6aS,6bR,16aR)-15-(3-fluorophenyl)-1,2,6a,6b,9,9,16a-heptamethyl-1,3,4,5,6,6a,6b,7,8,8a,9,16,16a,16b,17,18b-hexadecahydrochryseno[1,2-g][1,2,4]triazolo[5,1-b]quinazoline-4a(2H)-carboxylate (19)** White solid. Yield 50%, m.p. 130–132 °C. <sup>1</sup>H NMR (300 MHz,  $CDCl_3$ )  $\delta$  7.50 (s, 1H), 7.32 (d,  $J=5.1$  Hz, 2H), 7.21 (s, 1H), 5.74 (s, 1H), 5.24 (s, 1H), 4.10 (q,  $J=9.2$  Hz, 2H), 3.60 (s, 3H), 2.70–0.75 (m, 42H, protons in UA skeleton). MS (MALDI-TOF)  $m/z$  653 ( $M^+ + H$ ).

**Ethyl(1S,2R,4aS,6aS,6bR,16aR)-15-(3-bromophenyl)-1,2,6a,6b,9,9,16a-heptamethyl-1,3,4,5,6,6a,6b,7,8,8a,9,16,16a,16b,17,18b-hexadecahydrochryseno[1,2-g][1,2,4]triazolo[5,1-b]quinazoline-4a(2H)-carboxylate (20)** White solid. Yield 52%, m.p. 150–152 °C. <sup>1</sup>H NMR (300 MHz,  $CDCl_3$ )  $\delta$  7.71 (t,  $J=1.6$  Hz, 1H), 7.64–7.58 (m, 1H), 7.45 (dt,  $J=7.7$ , 1.3 Hz, 1H), 7.37 (d,  $J=7.8$  Hz, 1H), 5.77 (s, 1H), 5.24 (s, 1H), 4.12 (q,  $J=9.4$  Hz, 2H), 3.60 (s, 3H), 2.68–0.77 (m, 42H, protons in UA skeleton). MS (MALDI-TOF)  $m/z$  713 ( $M^+ + H$ ).

**Ethyl(1S,2R,4aS,6aS,6bR,16aR)-15-(furan-2-yl)-1,2,6a,6b,9,9,16a-heptamethyl-1,3,4,5,6,6a,6b,7,8,8a,9,16,16a,16b,17,18b-hexadecahydrochryseno[1,2-g][1,2,4]triazolo[5,1-b]quinazoline-4a(2H)-carboxylate (21)** White solid. Yield 52%, m.p. 140–142 °C. <sup>1</sup>H NMR (300 MHz, DMSO)  $\delta$  8.07 (d,  $J=1.1$  Hz, 1H), 7.31 (d,  $J=3.5$  Hz, 1H), 6.76 (dd,  $J=3.5$ , 1.8 Hz, 1H), 5.74 (s, 1H), 5.25 (s, 1H), 4.10 (q,  $J=9.2$  Hz, 2H), 3.53 (s, 3H), 2.45–0.76 (m, 42H, protons in UA skeleton). MS (MALDI-TOF)  $m/z$  625 ( $M^+ + H$ ). HRMS (ESI)  $m/z$  calcd for  $C_{39}H_{53}N_4O_3^+$  ( $M + H$ )<sup>+</sup> 625.41122, found 625.41071.

**Ethyl(1S,2R,4aS,6aS,6bR,16aR)-1,2,6a,6b,9,9,16a-heptamethyl-15-(naphthalen-2-yl)-1,3,4,5,6,6a,6b,7,8,8a,9,16**

**,16a,16b,17,18b-hexadecahydrochryseno[1,2-g][1,2,4]triazolo[5,1-b]quinazoline-4a(2H)-carboxylate (22)** White solid. Yield 54%, m.p. 134–136 °C. <sup>1</sup>H NMR (300 MHz, DMSO)  $\delta$  8.16 (s, 1H), 8.04 (d,  $J=8.9$  Hz, 3H), 7.72 (d,  $J=8.4$  Hz, 1H), 7.63 (d,  $J=5.1$  Hz, 2H), 5.77 (s, 1H), 5.08 (s, 1H), 4.12 (q,  $J=9.4$  Hz, 2H), 3.49 (s, 3H), 2.60–0.70 (m, 42H, protons in UA skeleton). MS (MALDI-TOF)  $m/z$  685 ( $M^+ + H$ ). HRMS (ESI)  $m/z$  calcd for  $C_{45}H_{57}N_4O_2^+$  ( $M + H$ )<sup>+</sup> 685.44760, found 685.44733.

**Ethyl(1S,2R,4aS,6aS,6bR,16aR)-1,2,6a,6b,9,9,16a-heptamethyl-15-(thiophen-2-yl)-1,3,4,5,6,6a,6b,7,8,8a,9,16,16a,16b,17,18b-hexadecahydrochryseno[1,2-g][1,2,4]triazolo[5,1-b]quinazoline-4a(2H)-carboxylate (23)** White solid. Yield 48%, m.p. 158–160 °C. <sup>1</sup>H NMR (300 MHz, DMSO)  $\delta$  7.82 (d,  $J=4.4$  Hz, 2H), 7.36–7.25 (m, 1H), 5.76 (s, 1H), 5.24 (s, 1H), 4.10 (q,  $J=9.2$  Hz, 2H), 3.53 (s, 3H), 2.59–0.75 (m, 42H, protons in UA skeleton). MS (MALDI-TOF)  $m/z$  641 ( $M^+ + H$ ).

### TNF- $\alpha$ , IL-6, and NO inhibitory activity

RAW264.7 cells were plated at  $3 \times 10^5$  cells/well in a 48-well microplate and incubated overnight. The cells were divided into six groups: normal group, positive group (DEX, 10  $\mu$ M), LPS group, and the test compounds groups (3, 10, or 30  $\mu$ M). Un-pretreated and un-stimulated RAW 264.7 cells were conducted as normal group. The positive group, LPS groups, and the test compounds groups were pretreated with LPS (1  $\mu$ g/mL) for 1 h. Then, the different concentrations of compounds were treated for 24 h. The culture supernatants were recovered and assayed using an ELISA kit (BD Biosciences, San Diego, CA, USA) to analyze the TNF- $\alpha$  productions according to the manufacturer's instruction. One-way ANOVA followed by Dunnett's multiple comparison test ( $*p < 0.05$ ,  $**p < 0.01$ ,  $***p < 0.001$ ) was used to detect the significance. Same to the TNF- $\alpha$  inhibitory activity, the effects of compounds **1–6**, **9**, **10**, **12**, **15**, and **18–23** on LPS-induced production of the inflammatory mediators NO and IL-6 by RAW 264.7 cells were evaluated.

### Molecular docking

All the calculations were performed using MOE 2008.10 software form Discovery studio 3.1 installed on 2.4G Core i5. To gain insight into the interaction between compound **3** and COX-2 enzyme, a docking simulation was performed using COX-2 (PDB ID: 5FDQ). The structures of compound **3**, UA, and **Celecoxib** were sketched in 2D and converted into 3D using the DS molecule editor. For the docking simulation, default values of quaternation, translation, and torsion steps were applied. The identification of ligand binding

modes was done iteratively by evaluating ligand conformations and estimating the binding energy of their interactions with these binding pockets. The binding pose with the top 5% highest scores was returned for further visual inspection [27]. The output poses of the ligands generated were analyzed based on the LibDock score function. Enzyme structures were checked for missing atoms, bonds, and contacts. Hydrogen atoms were added to the enzyme structure. Water molecules and bound ligands were manually deleted. The most stable molecular-docked model was selected according to the best scored conformation predicted by the MOE scoring function.

**Acknowledgements** This research was supported by the Natural Science Foundation of Jilin Province (No. 20190201077JC); The Health Department of Jilin Province (No. 2019ZC007); The Doctoral Foundation of Jilin Medical University (No. JYBS2018007); and The Jilin Province Students' Program for Innovation and Entrepreneurship Training (No. 202013706011).

## Compliance with ethical standards

**Conflict of interest** The authors state no conflict of interest.

## References

- Afonina IS, Zhong ZY, Karin M, Beyaert R (2017) Limiting inflammation—the negative regulation of NF- $\kappa$ B and the NLRP<sub>3</sub> inflammasome. *Nat Immunol* 18:861–869. <https://doi.org/10.1038/ni.3772>
- Manthiram K, Zhou Q, Aksentijevich I, Kastner DL (2017) The monogenic autoinflammatory diseases define new pathways in human innate immunity and inflammation. *Nat Immunol* 18:832–842. <https://doi.org/10.1038/ni.3777>
- Sherwood ER, Toliver-Kinsky T (2004) Mechanisms of the inflammatory response. *Best Pract Res Clin Anaesthesiol* 18:385–405. <https://doi.org/10.1016/j.bpa.2003.12.002>
- Lang Y, Chu FN, Shen DH, Zhang WGL, Zheng C, Zhu J, Cui L (2018) Role of inflammasomes in neuroimmune and neurodegenerative diseases: a systematic review. *Mediators Inflamm* 2018:1549549. <https://doi.org/10.1155/2018/1549549>
- Siti HN, Kamisah Y, Kamsiah J (2015) The role of oxidative stress, antioxidants and vascular inflammation in cardiovascular disease (a review). *Vascul Pharmacol* 71:40–56. <https://doi.org/10.1016/j.vph.2015.03.005>
- Stephenson J, Nutma E, Valk PVD, Amor S (2018) Inflammation in CNS neurodegenerative diseases. *Immunology* 154:204–219. <https://doi.org/10.1111/imm.12922>
- Karrasch T, Obermeier F, Straub RH (2014) Systemic metabolic signaling in acute and chronic gastrointestinal inflammation of inflammatory bowel diseases. *Horm Metab Res* 46:445–451. <https://doi.org/10.1055/s-0034-1374587>
- Kumar RS, Antonisamy P, Almansour AI, Arumugam N, Periyasami G, Altaf M, Kim HR, Kwon KB (2018) Functionalized spirooxindole-indolizine hybrids: stereoselective green synthesis and evaluation of anti-inflammatory effect involving TNF- $\alpha$  and nitrite inhibition. *Eur J Med Chem* 152:417–423. <https://doi.org/10.1016/j.ejmech.2018.04.060>
- Wang W, Wu YL, Chen XX, Zhang P, Li H, Chen LX (2019) Synthesis of new ent-labdane diterpene derivatives from andrographolide and evaluation of their anti-inflammatory activities. *Eur J Med Chem* 162:70–79. <https://doi.org/10.1016/j.ejmech.2018.11.002>
- Liu ZG, Tang LG, Zhu HP, Xu TT, Qiu CY, Zheng SQ, Gu YG, Feng JP, Zhang YL, Liang G (2016) Design, synthesis, and structure-activity relationship study of novel indole-2-carboxamide derivatives as anti-inflammatory agents for the treatment of sepsis. *J Med Chem* 59:4637–4650. <https://doi.org/10.1021/acs.jmedchem.5b02006>
- Chen GZ, Zhang YL, Liu X, Fang QL, Wang Z, Fu LL, Liu ZG, Wang Y, Zhao YJ, Li XK, Liang G (2016) Discovery of a new inhibitor of myeloid differentiation 2 from cinnamamide derivatives with anti-inflammatory activity in sepsis and acute lung injury. *J Med Chem* 59:2436–2451. <https://doi.org/10.1021/acs.jmedchem.5b01574>
- Albrecht W, Unger A, Bauer SM, Laufer SA (2017) Discovery of N-{4-[5-(4-Fluorophenyl)-3-methyl-2-methylsulfanyl-3H-imidazol-4-yl]-pyridin-2-yl}-acetamide (CBS-3595), a dual p38 $\alpha$  MAPK/PDE-4 inhibitor with activity against TNF $\alpha$ -related diseases. *J Med Chem* 60:5290–5305. <https://doi.org/10.1021/acs.jmedchem.6b01647>
- Imam F, Al-Harbi NO, Al-Harbi MM, Ansari MA, Zoheir KMA, Iqbal M, Anwer MK, Hoshani ARA, Attia SM, Ahmad SF (2015) Diosmin downregulates the expression of T cell receptors, pro-inflammatory cytokines and NF- $\kappa$ B activation against LPS-induced acute lung injury in mice. *Pharmacol Res* 102:1–11. <https://doi.org/10.1016/j.phrs.2015.09.001>
- Cohen J (2002) The immunopathogenesis of sepsis. *Nature* 420:885–891. <https://doi.org/10.1038/nature01326>
- Schulte W, Bernhagen J, Bucala R (2013) Cytokines in sepsis: potent immunoregulators and potential therapeutic targets—an updated view. *Mediat Inflamm* 2013:165974. <https://doi.org/10.1155/2013/165974>
- Checker R, Sandur SK, Sharma D, Patwardhan RS, Jayakumar S, Kohli V, Sethi G, Aggarwal BB, Sainis KB (2012) Potent anti-inflammatory activity of ursolic acid, a triterpenoid antioxidant, is mediated through suppression of NF- $\kappa$ B, AP-1 and NF-AT. *PLoS ONE* 7:e31318. <https://doi.org/10.1371/journal.pone.0031318>
- Nascimento PGGD, Lemos TLG, Bizerra AMC, Arriaga ÂMC, Ferreira DA, Santiago GMP, Braz-Filho R, Costa JGM (2014) Antibacterial and antioxidant activities of ursolic acid and derivatives. *Molecules* 19:1317–1327. <https://doi.org/10.3390/molecules19011317>
- Crosas-Molist E, Fabregat I (2016) Role of NADPH oxidases in the redox biology of liver fibrosis. *Redox Biol* 6:106–111. <https://doi.org/10.1016/j.redox.2015.07.005>
- Huang LH, Zheng YF, Lu YZ, Song CJ, Wang YG, Yu B, Liu HM (2012) Synthesis and biological evaluation of novel steroidal[17,16-d][1,2,4]triazolo[1,5-a]pyrimidines. *Steroids* 77:710–715. <https://doi.org/10.1016/j.steroids.2012.03.002>
- Wu J, Ma S, Zhang TY, Wei ZY, Wang HM, Guo FY, Zheng CJ, Piao HR (2019) Synthesis and biological evaluation of ursolic acid derivatives containing an aminoguanidine moiety. *Med Chem Res* 28:959–973. <https://doi.org/10.1007/s00044-019-02349-x>
- Aktan F (2004) iNOS-mediated nitric oxide production and its regulation. *Life Sci* 75:639–653. <https://doi.org/10.1016/j.lfs.2003.10.042>
- Li B, Yang YG, Chen LZ, Chen SC, Zhang J, Tang WJ (2017) 18 $\alpha$ -Glycyrrhetic acid monoglucuronide as an anti-inflammatory agent through suppression of the NF- $\kappa$ B and MAPK signaling pathway. *MedChemComm* 8:1498–1504. <https://doi.org/10.1039/c7md00210f>

23. Campbell IK, Roberts LJ, Wicks IP (2003) Molecular targets in immune-mediated diseases: the case of tumour necrosis factor and rheumatoid arthritis. *Immunol Cell Biol* 81:354–366. <https://doi.org/10.1046/j.0818-9641.2003.01185.x>
24. Spielmann S, Kerner T, Ahlers O, Keh D, Gerlach M, Gerlach H (2001) Early detection of increased tumour necrosis factor alpha (TNFalpha) and soluble TNF receptor protein plasma levels after trauma reveals associations with the clinical course. *Acta Anaesthesiol Scand* 45:364–370. <https://doi.org/10.1034/j.1399-6576.2001.045003364.x>
25. Wei ZY, Chi KQ, Wang KS, Wu J, Liu LP, Piao HR (2018) Design, synthesis, evaluation, and molecular docking of ursolic acid derivatives containing a nitrogen heterocycle as anti-inflammatory agents. *Bioorg Med Chem Lett* 28:1797–1803. <https://doi.org/10.1016/j.bmcl.2018.04.021>
26. Zheng XJ, Li CS, Cui MY, Song ZW, Bai XQ, Liang CW, Wang HY, Zhang TY (2020) Synthesis, biological evaluation of benzothiazole derivatives bearing a 1,3,4-oxadiazole moiety as potential anti-oxidant and anti-inflammatory agents. *Bioorg Med Chem Lett* 30:127237. <https://doi.org/10.1016/j.bmcl.2020.127237>
27. Lui HK, Gao W, Cheung KC, Jin WB, Sun N, Kan JWY, Wong ILK, Chiou JC, Lin DC, Chan EWC, Leung YC, Chan TH, Chen S, Chan KF, Wong KY (2019) Boosting the efficacy of anti-MRSA  $\beta$ -lactam antibiotics via an easily accessible, noncytotoxic and orally bioavailable FtsZ inhibitor. *Eur J Med Chem* 163:95–115. <https://doi.org/10.1016/j.ejmech.2018.11.052>

**Publisher's Note** Springer Nature remains neutral with regard to jurisdictional claims in published maps and institutional affiliations.